

# Observed features of GPS Block IIF satellite yaw maneuvers and corresponding modeling

Da Kuang<sup>1</sup>  · Shailen Desai<sup>1</sup> · Aurore Sibois<sup>1</sup>

Received: 14 March 2016 / Accepted: 12 August 2016 / Published online: 26 August 2016  
© Springer-Verlag Berlin Heidelberg (outside the USA) 2016

**Abstract** After comparing the modeled and the estimated yaw angles during yaw maneuvers for eight Block IIF Global Positioning System satellites over 1 year, we have observed discrepancies between the yaw directions in the vicinity of zero beta angle. Two features of the turn maneuvers are extracted after analysis of the observed differences: (1) The noon-turns reverse yaw direction when the beta angle falls between  $[-0.7^\circ, 0^\circ]$ ; (2) midnight-turns always take the direction that completes  $<180^\circ$  of total yaw. We present the approach implemented to account for the discrepancies between the observed and modeled yaw attitudes. In particular, an empirical beta angle bias is applied in the noon-turn model to correct the yaw direction error, and a short-route constraint is applied in the midnight-turn model for more robust performance.

**Keywords** GPS · Block IIF · Yaw attitude · IGS clock solution

## Introduction

Accurate knowledge of the attitude, or orientation, of the Global Positioning System (GPS) satellites in space is essential for precise GPS orbit determination and GPS-based high-precision applications. The attitude model of the GPS satellites affects the computation of measurement geometry through variations of the transmitter phase center location (Bar-Sever et al. 1996) and carrier phase

measurement wind-up (Wu et al. 1993). It also affects the modeling of the solar radiation pressure force acting on the GPS satellites due to the changes in illumination geometry (Fliegel et al. 1992; Kuang et al. 1996; Ziebart and Dare 2001). Nominal (or ideal) GPS satellite attitude points the transmitter antennas toward the earth center and the solar panels toward the sun all the time through continuous yaw (rotation around satellite body-fixed  $Z$  axis) and pitch (rotation around body-fixed  $Y$  axis) control processes (Fliegel et al. 1992). For the majority of time, this nominal attitude model fits actual GPS measurements well. However, during eclipsing season when the angle between the satellite orbital plane and the sun, the so-called  $\beta$  angle, is small (typically below  $4^\circ$ ), the physical GPS satellite yaw attitude rate cannot keep up with what is expected from the nominal model. Besides, for Block II/IIA satellites, the loss of tracking of the sun in the shadow also causes the satellite to yaw at its maximum rate (Bar-Sever et al. 1996). All these effects result in the actual satellite attitude deviating from nominal attitude. Numerous investigations over the last two decades have shown that the GPS attitude models perform inferiorly during eclipsing season, and various efforts have been devoted to improving their performance (Bar-Sever 1996; Kouba 2009; Dilssner 2010). We describe our approach to model the yaw attitude of the Block IIF GPS satellites in eclipse.

As shown in Fig. 1, the yaw angle,  $\Psi$ , of a GPS satellite is defined as the angle between the satellite body-fixed  $X$  axis and the orbit plane, with a sign opposite to that of  $\beta$  angle (Bar-Sever 1996). The angle between the sun and the satellite viewed at the earth center is  $\varepsilon$ . The orbital angle,  $\mu$ , lies in the orbit plane and increases with orbital motion starting from the orbit midnight direction. The physical yaw angle of different types of GPS satellites deviates from the nominal model during eclipses in slightly different

✉ Da Kuang  
dakuang@jpl.nasa.gov

<sup>1</sup> Jet Propulsion Laboratory, California Institute of Technology, Pasadena, CA, USA

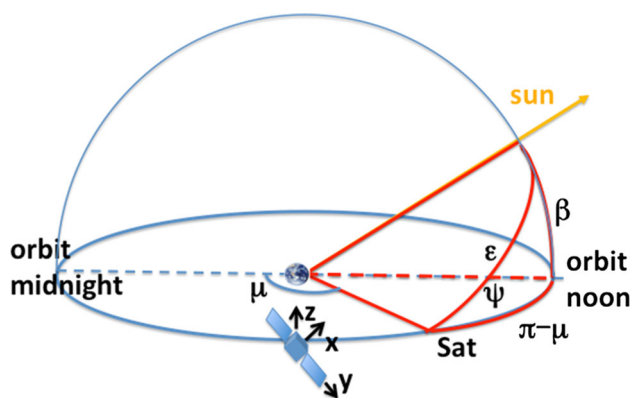


Fig. 1 GPS satellite yaw attitude geometry

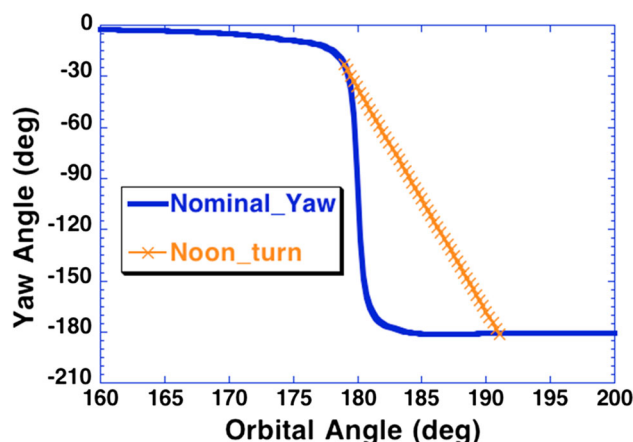


Fig. 3 Yaw angle of GPS satellites during noon-turn maneuvers

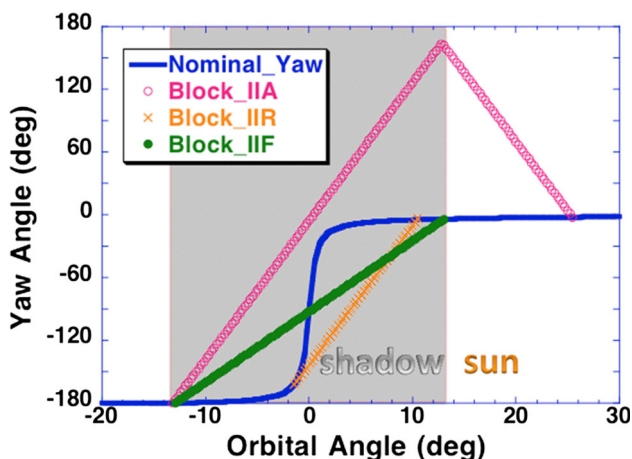


Fig. 2 Yaw angle of GPS satellites during midnight-turn maneuvers

ways. Figure 2 illustrates the yaw angles of different blocks of GPS satellites as functions of orbital angle. After a yaw bias was implemented in the attitude control subsystem (ACS) on Block IIA GPS satellites in 1994, these satellites yaw at their maximum rate throughout the entire umbra shadow, then recover the nominal attitude after exiting the shadow with either continuing or opposite yaw as is necessary for the recovery (Bar-Sever et al. 1996). Block IIR GPS satellites start to yaw at their maximum rate when the nominal rate reaches the physical limit, until the nominal yaw is recovered (Kouba 2009). In contrast, the newer Block IIF GPS satellites yaw at a rate lower than their maximum rate throughout the umbra shadow crossing, as observed by Dilssner (2010). As first described by Bar-Sever (1996), all GPS satellites perform noon-turn maneuvers in the same way and follow the approach of the midnight-turn of the Block IIR satellites (Fig. 3).

With the Reversed Kinematic Precise Point Positioning (RPPP) technique (Dilssner 2010), the actual yaw angle of a GPS satellite can be estimated using pseudorange and carrier phase measurements from a network of ground

receivers, at least for those satellites with a significant transmitter phase center offset from their yaw axis. By comparing the estimated yaw angle with the expected model, Dilssner et al. (2011) observed that the noon-turn of the Block IIF satellites manifests in the wrong direction for a small negative  $\beta$  angle as much as  $-0.9^\circ$ . Kouba (2013) found that the satellite ACS yaw bias of  $-0.5^\circ$  could fully explain the wrong turn for negative  $\beta$  between  $-0.5^\circ$  and  $0^\circ$ . A routine RPPP process (Weiss et al. 2012) is also used at the Jet Propulsion Laboratory (JPL) to measure and monitor the actual attitude of Block IIA and IIF GPS satellites. We independently analyzed the accumulated cases of discrepancies between our Block IIF model-computed yaw angles and those observed by JPL’s RPPP process for Block IIF satellites over a period of 1 year. Our goal is to gain a better understanding of the attitude control process and subsequently improve the attitude model for the Block IIF satellites.

### Modeled and observed yaw maneuvers for block IIF satellites

In JPL’s software (GNSS-Inferred Positioning System, GIPSY), the yaw angle,  $\Psi(t)$ , for midnight-turns of Block IIF satellites is modeled as:

$$\Psi(t) = (t - t_s) \cdot (\Psi(t_e) - \Psi(t_s)) / (t_e - t_s) \tag{1}$$

where the maneuver starting time  $t_s$  and ending time  $t_e$  are the umbra shadow entry and exit times, respectively. For noon-turns, the model is the same as the Block IIA noon-turn model developed by Bar-Sever (1996):

$$\Psi(t) = \Psi(t_s) - \text{SIGN}(R, \beta) \cdot (t - t_s) \tag{2}$$

where  $R$  is the physical limit (maximum) of the satellite’s yaw rate. SIGN is the function taking the value from  $R$  and the sign from  $\beta$ . Kouba (2009) uses a slightly different

expression for noon-turns of both Block IIA and Block IIR satellites:

$$\Psi(t) = \Psi(t_s) + \text{SIGN}(R, \Psi'(t_s)) \cdot (t - t_s) \tag{3}$$

where  $\Psi'$  is the yaw rate (time derivative of  $\Psi$ ).

The two models, Eqs. (2) and (3), represent two slightly different logics: one based on which side the sensor sees the sun, the other based on momentum, i.e., which way the satellite has been turning. Despite this difference, however, they give essentially identical results in practice. Figure 4 shows the yaw angle and rate computed from the nominal yaw model for  $\beta$  angles ranging from  $-0.7^\circ$  to  $0.7^\circ$ . Both the yaw angle and yaw rate change sign when  $\beta$  angle crosses the border of  $\beta = 0^\circ$ . When an ACS yaw bias of  $-0.5^\circ$  is introduced for Block IIF satellites, as noted by Kouba (2013), the corresponding yaw angle and rate computed from the biased yaw model, described by Eqs. (3) and (5) of Bar-Sever (1996), are shown in Fig. 5. Now, both the yaw angle and yaw rate change sign when  $\beta$  angle crosses the line of  $\beta = -0.5^\circ$ , reversing their sign

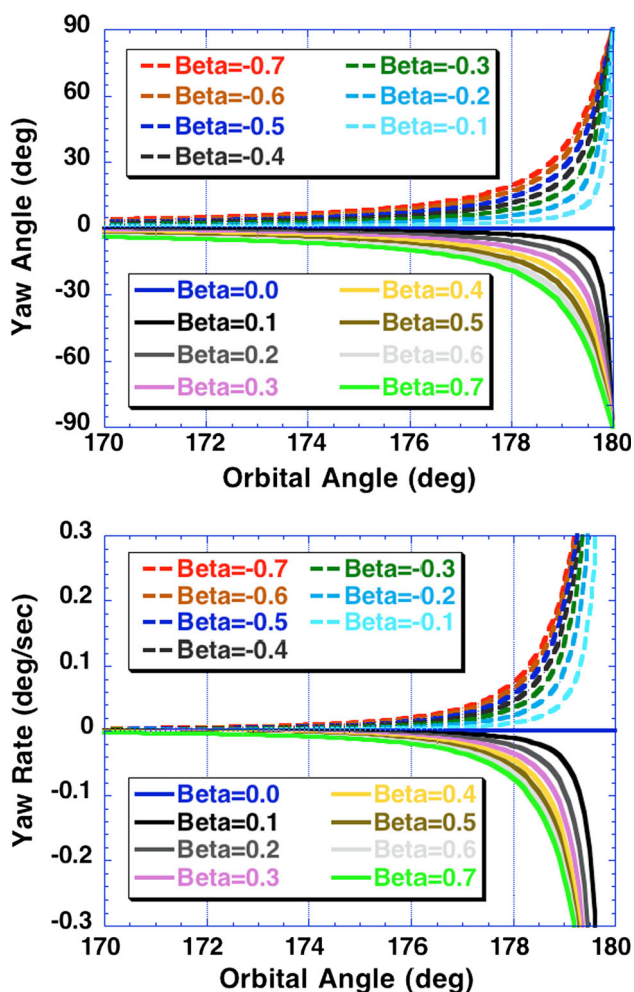


Fig. 4 Yaw angle and rate of the nominal yaw attitude in the vicinity of orbit noon

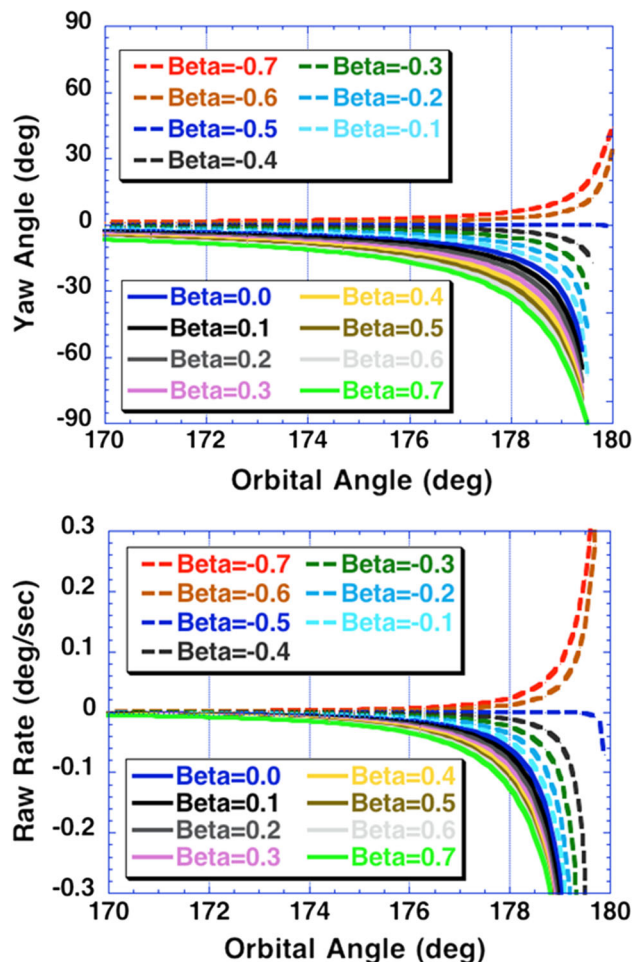


Fig. 5 Yaw angle and rate of biased yaw attitude in the vicinity of orbit noon

from the nominal value over a small interval  $[-0.5, 0]$  of  $\beta$  angle, as if the “apparent”  $\beta$  angle is shifted by  $-0.5^\circ$ .

The GPS yaw attitude estimated using the RPPP technique (Dilssner 2010; Weiss et al. 2012) is a completely independent evaluation of the yaw angle without using any of the aforementioned models. It can be used to monitor the actual yaw attitude status of GPS satellites as well as to validate the yaw attitude models. For Block IIF satellites, which have a 40 cm phase center offset from the yaw axis, our estimated yaw angles typically show agreement with the modeled angles within  $5^\circ$ , consistent with Dilssner’s observations (2010). However, approximately twice a year the estimated yaw attitude shows episodes of reversed yaw directions with respect to the model, for both midnight-turn and noon-turn maneuvers over a small range of  $\beta$  angles.

Figure 6 shows an example, for GPS satellite vehicle number (SVN) 67 on 11 February 2015, in which both observed midnight- and noon-turns demonstrate opposite yaw directions from the model. The  $\beta$  angle for this satellite varies between  $-0.28^\circ$  and  $0.5^\circ$  during that day.

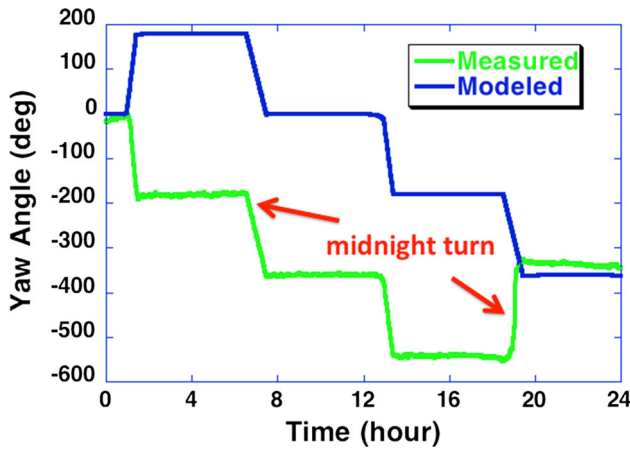


Fig. 6 Discrepancies between observed and modeled yaw maneuver directions for GPS67 on 11 February 2015

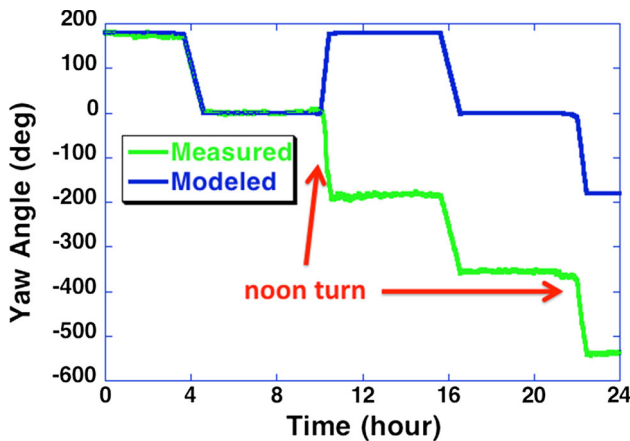


Fig. 7 Observed reversed sign of noon-turn direction with respect to model for GPS63 on 11 February 2015

Figure 7 shows another example, for GPS SVN 63 on the same day, where one case of a discrepancy in yaw direction between observed and modeled noon-turn is demonstrated, when the  $\beta$  angle changes from  $-0.26^\circ$  to  $0.21^\circ$  during the day.

### Features of observed discrepancies and empirical correction to the models

We collected the observed discrepancies of yaw directions for eight Block IIF GPS satellites over a period of more than 1 year (October 2014–November 2015) and analyzed these discrepancies in various parameter domains in an attempt to characterize their features and understand the cause. With a few exceptions, the observed discrepancies can be summarized into two features:

1. Noon-turns reverse yaw direction when the  $\beta$  angle falls in the region of  $[-0.7^\circ, 0^\circ]$ , as shown in Fig. 8.

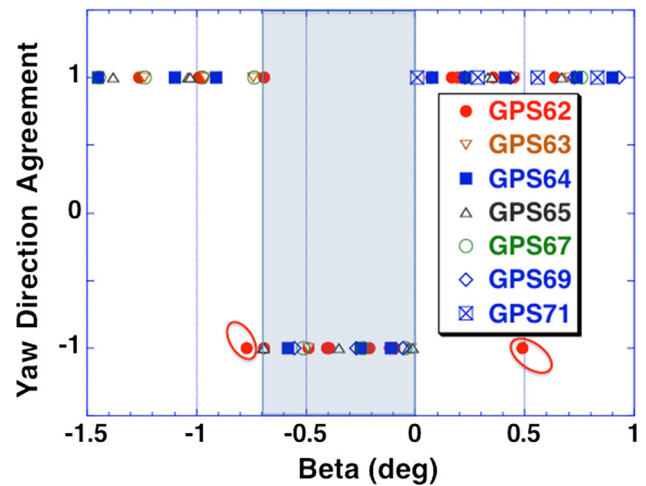


Fig. 8 Correlation between noon-turn direction discrepancy and  $\beta$  angle. A value of 1 indicates agreement between observed and modeled yaw direction, while a value of  $-1$  indicates disagreement. Two exceptions occur over the considered period and are highlighted by the red circles

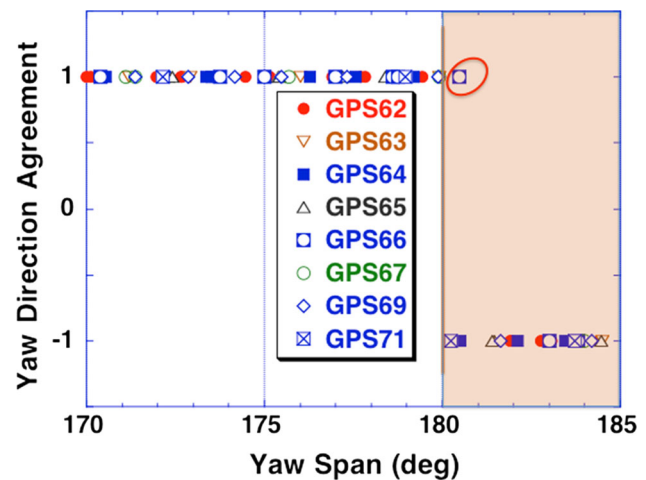


Fig. 9 Correlation between midnight-turn direction discrepancy and total yaw span. A value of 1 indicates agreement between observed and modeled yaw direction, while the value of  $-1$  indicates disagreement. The exception observed over the considered period is highlighted by the red circle

According to Fig. 5,  $0.5^\circ$  out of the  $0.7^\circ$  can be explained by the omission of the “apparent”  $\beta$  angle shift (in Eq. 2) or “bias rate” (in Eq. 3) introduced by the  $-0.5^\circ$  of yaw bias. The remainder can be caused by any error in evaluating  $\beta$  in Eq. (2), including errors in the evaluation of the noon-turn starting time  $t_s$

2. Midnight-turns always take the direction that completes  $<180^\circ$  of total yaw, as shown in Fig. 9. In theory, the nominal total yaw angle  $\Psi(t_e) - \Psi(t_s)$  would never be greater than  $180^\circ$ . However, at very small  $\beta$  angle, this total yaw is very close to  $180^\circ$  and a small error in evaluating  $t_e$  and  $t_s$  (using osculating orbital elements)

can cause the model-computed yaw to be slightly  $>180^\circ$ , especially when combined with the effects of the yaw bias. This otherwise harmless small numerical error, when manifesting into a wrong turn direction, causes an accumulated yaw angle error of  $360^\circ$  at the end of the midnight-turn maneuver.

Based on these observed features, we add the following empirical corrections to the yaw model for the Block IIF satellites during eclipsing season:

1. A bias of  $0.7^\circ$  is applied to the  $\beta$  angle in the noon-turn direction decision making:

$$\Psi(t) = \Psi(t_s) - \text{SIGN}(R, \beta + 0.7) \cdot (t - t_s). \tag{4}$$

2. A short-route constraint is applied in the midnight-turn direction decision making to force it to turn  $<180^\circ$ :

$$\Psi(t) = (t - t_s) \cdot \Delta\Psi / (t_e - t_s) \tag{5}$$

where

$$\begin{aligned} \Delta\Psi &= (\Psi(t_e) - \Psi(t_s)) && \text{for } |\Psi(t_e) - \Psi(t_s)| \leq 180^\circ \\ \Delta\Psi &= (\Psi(t_e) - \Psi(t_s)) + 360^\circ && \text{for } \Psi(t_e) - \Psi(t_s) < -180^\circ \\ \Delta\Psi &= (\Psi(t_e) - \Psi(t_s)) - 360^\circ && \text{for } \Psi(t_e) - \Psi(t_s) > 180^\circ \end{aligned}$$

With the revised yaw model for Block IIF satellites, most of the wrong turn directions in Figs. 8 and 9 are corrected, except for the cases circled in red. Post-fit data residuals from their precise orbit determination (POD) become smaller, and orbit and clock solutions are smoother around turn events. Figure 10 shows all carrier phase post-fit data residuals

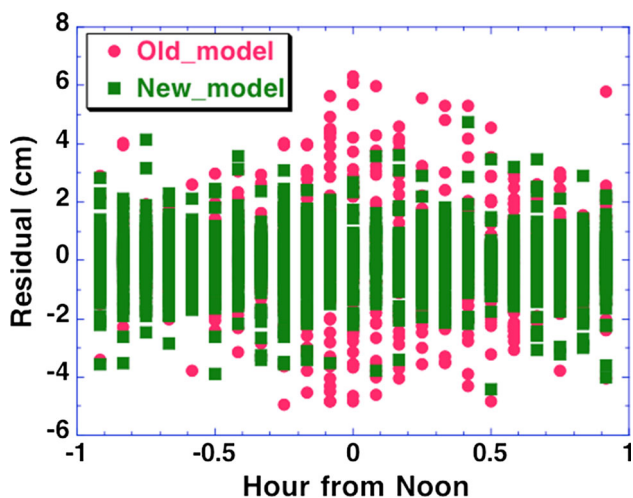


**Fig. 10** Carrier phase data post-fit residuals for GPS63 and GPS67 around noon-turn events on 11 February 2015 are smaller when applying our revised yaw model

associated with GPS63 and GPS67 around their noon-turn events on 11 February 2015. With the revised yaw attitude model (in green), the post-fit residuals are significantly reduced during the maneuvers that last for about 50 min. Figure 11 shows the smoothness of the clock solutions for GPS63 and GPS67 around their noon-turn events on 11 February 2005. A linear trend and once-per-orbit variation have been removed from the estimated transmitter clock correction. With the old yaw attitude model (in red), there are clear changes in clock correction at the decimeter level during the noon-turn maneuver, which is about one cycle of ionosphere-free carrier phase measurement change. With our revised model, these abrupt clock changes disappear.

A wrong turn direction in the yaw maneuver model manifests its effect in the measurement model in two different ways: the lever arm due to the phase center offset and the phase windup due to the spin of the dipoles. The lever arm swing has the same effect on both pseudorange and carrier phase measurements but different effect on receivers at different ground locations. This error cannot be easily absorbed into a single parameter such as transmitter clock, but spreads into various domains if not all into post-fit data residuals (Fig. 10).

Windup error due to an incorrect yaw model of a GPS satellite is common to measurements in all associated ground stations. As a result, these errors are mostly absorbed into transmitter clock estimates and cause possible biases in pseudorange measurement residuals because the carrier phase measurement data are typically weighted 100 times higher than pseudorange in the estimation problem. Pseudorange measurements themselves do not have windup errors.

Because of the continuity of carrier phase measurements and the adjustability of phase biases to account for unmodeled biases in the carrier phase measurements, clock errors due to the mis-modeling of the yaw turn direction in

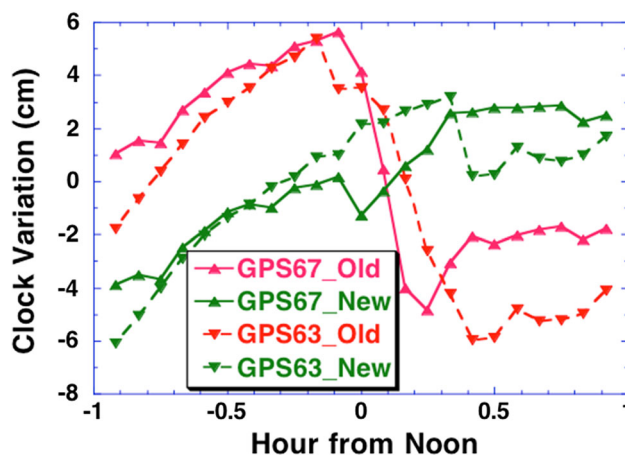


**Fig. 11** De-trended clock solutions for GPS63 and GPS67 around noon-turn events on 11 February 2015 are smoother when applying our revised yaw model

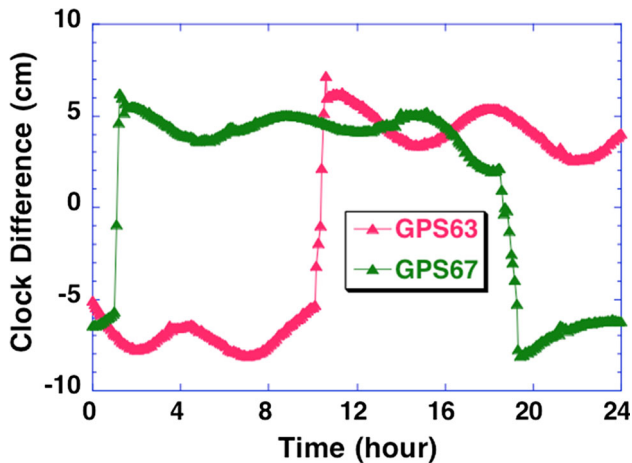


**Fig. 12** Differences in transmitter clock solutions between using the old and revised yaw attitude models on 11 February 2015. GPS63 experienced one reversed turn, while GPS67 experienced two

the POD process can manifest as a bias spreading over a much longer period of time than the turn event itself. Once introduced, the clock error may manifest over the remainder of the orbit solution arc until an opposite turn direction error occurs to unwind it. Figure 12 shows the differences between the estimated transmitter clocks when using old and revised yaw maneuver models. GPS67 had two mis-modeled turn maneuvers on 11 February 2015, and during the time interval between these two maneuvers the transmitter clock estimation was biased by about 10 cm. GPS63 had only one mis-modeled turn maneuver on that day, and the bias in the estimated transmitter clock remained all the way till the end of the orbit solution arc.

This error in the clock estimation is a systematic error depending mainly on the yaw attitude model but not sensitive to other factors used in the POD process. For example, we have verified that various analysis centers of the International GNSS Service (IGS) (Dow et al. 2009) have similar clock errors in their products even though different data set and software are used to generate their products, as shown in Fig. 13. As a result, this error does not average out in the IGS combination process but remains in the final IGS product.

## Summary

Through the comparison between modeled and observed yaw attitudes for GPS satellites, we have characterized two features of the attitude behavior of Block IIF GPS satellites during yaw maneuvers. The origin of these features can be partly explained by the ACS yaw bias implemented in the Block IIF satellites. The remainder may be caused by errors in evaluating parameters such as maneuver starting time and beta angle, which may differ by satellites and

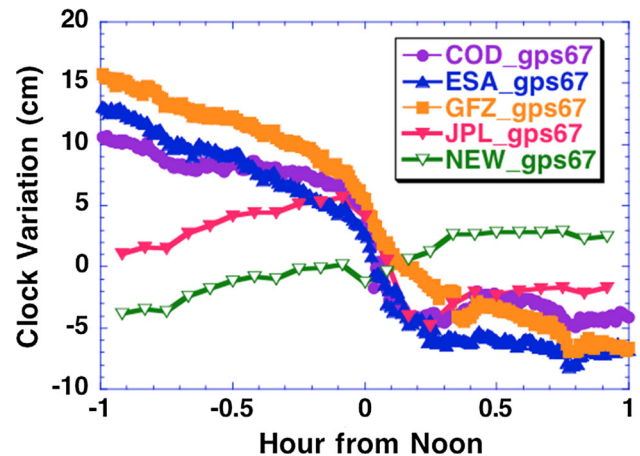


**Fig. 13** Smoothness of clock solutions from IGS centers for GPS67 around its noon-turn event on 11 February 2015

software that use different evaluating algorithms. We did notice similar beta-angle-dependent behavior for Block IIA satellites as well during noon-turn maneuvers. With a positive ACS yaw bias of  $0.5^\circ$ , most Block IIA satellites' noon-turn direction errors occur in the beta angle region of  $[0^\circ, 1^\circ]$ . We do not address the IIA yaw model because it is more complicated and fewer RPPP solutions are available now for eclipsing IIA satellites. However, the few available observations strengthened our belief that the ACS yaw bias plays a fundamental role in the GPS satellites yaw maneuver behavior.

Based on these characterizations, we implemented a revised yaw maneuver model for Block IIF satellites. It shows improved performance when applied to network solutions of the GPS satellites. Most notably, post-fit data residuals are reduced, and clock solutions are smoother near the yaw maneuvers. The revised model significantly narrows the beta angle region in which the performance of the yaw model is uncertain. However, this uncertainty region still exists. Because of the binary nature of the switch in directions, it is challenging to model the yaw turn 100 % accurately. Any error in orbital angle evaluation (for noon-turn) or shadow boundary evaluation (for midnight-turn) can result in the wrong decision of the turn direction and cause  $360^\circ$  of phase measurement error.

Improving GPS satellite yaw models is an ongoing effort. It is very challenging to predict the correct turn direction a priori or to determine it in near real-time. However, post-processing (e.g., the RPPP process) has the potential to provide this information. The post-process corrected GPS attitude knowledge could then be fed back into the POD process, and possibly added as an IGS product (Colombo 2016), to help users improve the performance of precise positioning applications.

**Acknowledgments** The work described is carried out by the Jet Propulsion Laboratory, California Institute of Technology, under contract with the National Aeronautics and Space Administration. We are thankful to Yoaz Bar-Sever for helpful discussions on the original Block IIF GPS satellite yaw model. The effort by our colleagues in creating and maintaining the routine RPPP solutions of GPS satellites yaw attitude is gratefully appreciated. We also thank the two anonymous reviewers whose comments and suggestions broadened our knowledge about related studies in the IGS community and made this paper more robust.

## References

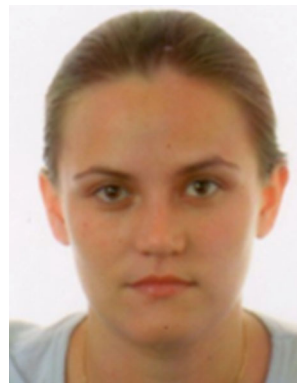
- Bar-Sever Y (1996) A new model for GPS yaw attitude. *J Geod* 70(11):714–723
- Bar-Sever YE, Bertiger WI, Davis ES (1996) Fixing the GPS bad attitude: modeling GPS Satellite yaw during eclipse seasons. *Navigation* 43(1):25–39
- Colombo OL (2016) Testing a reverse kinematic point positioning technique for possible operational use in GPS data analysis at NASA's Goddard space flight center. IGS workshop 2016, Sydney
- Dilssner F (2010) GPS IIF-1 satellite antenna phase center and attitude modeling. *Inside GNSS* 5:59–64
- Dilssner F, Springer T, Enderle W (2011) GPS IIF yaw attitude control during eclipse season, AGU Fall Meeting, San Francisco, 9 Dec. 2011. [http://acc.igs.org/orbits/yaw-IIF\\_ESOC\\_agu11.pdf](http://acc.igs.org/orbits/yaw-IIF_ESOC_agu11.pdf)
- Dow JM, Neilan RE, Rizos C (2009) The International GNSS Service in a changing landscape of Global Navigation Satellite Systems. *J Geod* 83(3–4):191–198. doi:10.1007/s00190-008-0300-3
- Fliegel HF, Gallini TE, Swift ER (1992) Global Positioning System radiation force model for geodetic applications. *J Geophys Res* 97:559–568
- Kouba J (2009) A simplified yaw-attitude model for eclipsing GPS satellites. *GPS Solut* 13(1):1–12
- Kouba J (2013), Noon turns for deep eclipsing Block IIF GPS satellites, a note prepared for IGS ACs, dated 19 Dec, 2013 [IGS-ACS-930 Mail]
- Kuang D, Rim HJ, Schutz BE, Abusali PAM (1996) Modeling GPS satellite attitude variation for precise orbit determination. *J Geod* 70(9):72–580
- Weiss J, Bar-Sever Y, Bertiger W, Desai S, Harvey N, Sibthorpe A (2012) Modeling and characterization of the GPS Block II/IIA/IIF attitude. IGS Workshop 2012, Olsztyn
- Wu JT, Wu SC, Hajj GA, Bertiger WI, Lichten SM (1993) Effects of Antenna Orientation on GPS Carrier Phase. *Manuscripta Geod* 18(2):91–98
- Ziebart M, Dare P (2001) Analytical solar radiation pressure modeling for GLONASS using a pixel array. *J Geod* 75:587–599



**Da Kuang** is a Senior Research Technologist in the Near-Earth Tracking Applications Group at the Jet Propulsion Laboratory. He received his Ph.D. degree in Aerospace Engineering from the University of Texas at Austin in 1995. His research activities include precise orbit determination for GNSS satellites and using GNSS tracking data for precise orbit determination of low-Earth orbiters.



**Shailen Desai** received his Bachelor's degree in Aeronautical and Astronautical Engineering from Purdue University in 1990, and his Master's and Ph.D. in Aerospace Engineering Sciences from the University of Colorado in 1992 and 1996. He has been with the Jet Propulsion Laboratory since 1996. His research interests include satellite geodesy, satellite altimetry and precise orbit determination.



**Aurore Sibois** is a Research Technologist in the Near-Earth Tracking Applications Group at the Jet Propulsion Laboratory. She received an engineering degree from ESIEE Paris (France) in 2005, a master's degree in Radio and Space Science from Chalmers University of Technology (Sweden) in 2005 and a Ph.D. in Aerospace Engineering Sciences from the University of Colorado at Boulder in 2011. Her research interests include GNSS precise orbit determination and precise determination of the Earth rotation parameters using GNSS.